

## Monte Carlo renormalization-group study of the three-dimensional Ising model

Clive F. Baillie

*Physics Department, University of Colorado, Boulder, Colorado 80309*

Rajan Gupta

*T-8, MS-B285, Los Alamos National Laboratory, Los Alamos, New Mexico 87545*

Kenneth A. Hawick and G. Stuart Pawley

*Physics Department, Edinburgh University, Edinburgh, EH9 3JZ, Scotland*

(Received 25 October 1991; revised manuscript received 5 December 1991)

We present results of a Monte Carlo renormalization-group study of the three-dimensional Ising model on  $64^3$  and  $128^3$  simple-cubic lattices. The eigenvalues of a linearized transformation matrix, constructed with the use of 53 even operators and 46 odd operators, are shown to be free of truncation errors. Our estimate of the critical coupling is  $0.221\,652 \pm 0.000\,003 \pm 0.000\,001$  where the first error is statistical and the second due to the finite number of blocking steps. The results for the relevant exponents are  $\nu = 0.624(2)$  and  $\eta = 0.026(3)$ . This estimate for  $\nu$  lies  $2-3\sigma$  below that obtained from other methods. The correction-to-scaling exponent is found to lie in the range  $\omega = 0.8-0.85$ . We also find that the subleading magnetic exponent is relevant and present evidence that it corresponds to a redundant eigenvector of the majority-rule blocking transformation.

### I. INTRODUCTION

In this paper we present results of extensive simulations of the critical behavior of the three-dimensional (3D) Ising model using the Monte Carlo renormalization-group (MCRG) method. The analysis has been done on  $64^3$  and  $128^3$  lattices. This allows us to compare our  $64^3$  data with previous results (Pawley *et al.*<sup>1</sup> and Blöte *et al.*<sup>2</sup>), while the  $128^3$  simulations provide additional results. Our calculation improves on previous MCRG estimates for the critical coupling  $K_{NN}^c$  and for the exponents  $\nu$ ,  $\omega$ , and  $\eta$ .

We discuss how to reduce the three major sources of systematic errors in MCRG calculations. These are (a) truncation errors, (b) lack of convergence, and (c) finite-size errors at higher blocking levels. The statistical sample consists of 100-K (140-K) measurements on  $64^3$  ( $128^3$ ) lattices. Most of the data are generated using the single-cluster update for which the dynamical critical exponent has been shown to be  $z = 0.28$ .<sup>3</sup> Nevertheless, one of the largest remaining source of errors in this calculation is the statistics.

We present evidence that the subleading odd operator is a redundant operator with eigenvalue greater than unity. This relevant redundant operator associated with the  $2^3$  blocking (majority rule) is not responsible for the slow convergence of MCRG calculations. The rate of convergence is governed by the correction-to-scaling exponent  $\omega$ , for which our estimate is the range  $0.80-0.85$ .

We make a detailed comparison of results for  $K_{NN}^c$ ,  $\nu$ , and  $\eta$  with those obtained using other methods such as series expansion, finite-size scaling, etc. Our results for  $\nu$  lies  $(2-3)\sigma$  below non-MCRG estimates. We consider this difference significant. Based on our data, we conjecture that once the statistical errors are brought under

control, simulations on  $64^3$ ,  $128^3$ , and  $256^3$  lattices will allow us to extrapolate reliably to infinite volume and provide very accurate results.

This paper is organized as follows: In Sec. II we review the essentials of the MCRG method. The details of implementation of the program on the AMT DAP (Distributed Array Processor) and of our update and measurement parameters are given in Sec. III. The analysis leading to an improved estimate of the nearest-neighbor critical coupling  $K_{NN}^c$  is presented in Sec. IV, for the thermal exponent  $\nu$  in Sec. V, and for the magnetic exponent  $\eta$  in Sec. VI. In Sec. VII we analyze Wilson's method to determine the leading exponents using renormalization-group flows. A discussion of subleading (correction-to-scaling) exponents is given in Sec. VIII, where we also present evidence that the subleading operator in the odd sector is redundant. Finally, in Sec. IX we make a comparison of results obtained with different methods including  $\epsilon$  expansion, series analysis, finite-size scaling supplemented with the histogram method, and the transfer-matrix method. We end with conclusions and future outlook in Sec. X. Throughout this paper the quoted errors always refer to the last decimal place unless explicitly stated.

### II. MCRG METHOD

The Monte Carlo renormalization-group (MCRG) method combines Monte Carlo (MC) simulation techniques<sup>4</sup> with a renormalization-group (RG) analysis of the critical properties of statistical-mechanics models.<sup>5</sup> Key conceptual ingredients of the MCRG method were provided by Ma<sup>6</sup> and Kadanoff<sup>6</sup> and the method was developed into a calculational tool in 1979 by Wilson<sup>7</sup> and Swendsen.<sup>7</sup> The basic idea of the renormalization

group is that near a critical point the correlation length diverges and the long-distance properties of a system are not affected by details at the microscopic level. Thus short-wavelength fluctuations may be integrated out, transforming the original system into another one with fewer degrees of freedom. The effect of integrating out the short-wavelength fluctuations is to renormalize the couplings. Critical exponents are derived from analyzing how the couplings change under such coarse graining.

In practice, the integration cannot be done exactly, and in numerical simulations the coarse graining is done in small discrete steps. Such approximate transformations, called blocking transformations, are designed to preserve the long-distance physics of the model. There is considerable freedom in how to approximately carry out the integration over the short-distance fluctuations, and one expects all sensible transformations to give the same results.

Monte Carlo simulations are used to generate configurations of spin variables with a starting Hamiltonian lying as close as possible to the infinite lattice critical surface. Given these configurations, one implements the scale transformations numerically by dividing the lattice into "blocks" and averaging the variables in each block to define the "block variable." How well a given blocking scheme approximates integration over a fraction of the variables is controlled by the precise definition of the averaging procedure.

Different blocking transformations can be constructed because of the freedom in defining the size and shape of the block (usually denoted by the scale factor of the transformation) and the averaging procedure. For regular hypercubic lattices, blocking transformations by a scale factor  $b$  reduce the volume of a  $d$ -dimensional system by  $b^d$ , which is also usually equal to the number of variables in a block. We use the majority-rule transformation for the 3D Ising model, dividing the simple-cubic lattice of spins into  $2 \times 2 \times 2$  blocks ( $b=2$ ) and assigning the values  $+1$  or  $-1$  to the block spin, depending on the sign of the sum of the spins in the block. When the sum is zero, the block spin is assigned the value  $\pm 1$  with equal probability.

To generate the RG flow, one repeats the blocking procedure a number of times. At each blocking the lattice volume decreases by a factor  $b^d$ ; nevertheless, each blocked lattice holds the same long-distance physics information as the original simulated lattice, but is a successively coarser representation of it.

To analyze the effect of blocking, it is convenient to write the starting Hamiltonian (original simulated system) in its most general form:

$$\mathcal{H} = \sum_{\alpha} K_{\alpha} S_{\alpha} , \quad (2.1)$$

where the interactions  $S_{\alpha}$ 's are combinations of the spins and the  $K_{\alpha}$ 's are the corresponding coupling constants. The sum is over all possible interactions that exist on a lattice of a given size. The RG transformation  $\mathcal{R}_b$  produces another system corresponding to the renormalized Hamiltonian

$$\mathcal{H}' = \sum_{\alpha} K'_{\alpha} S'_{\alpha} = \mathcal{R}_b \mathcal{H} , \quad (2.2)$$

parametrized in terms of a different set of coupling constants  $\{K'_{\alpha}\}$ . The interactions  $S'_{\alpha}$  are combinations of the block spins. Thus the RG transformation is a map in the space of coupling constants, and theories connected by a RG transformation describe the same long-distance physics if they lie in the domain of attraction of the critical fixed point  $\mathcal{H}^* = \mathcal{R}_b \mathcal{H}^*$ . For this reason MCRG simulations are most reliable when the starting Hamiltonian lies on the critical surface since then the RG flow converges to the relevant fixed point. For more details on these points, we direct the reader to Refs. 8 and 9.

In numerical simulations the condition for success of the MCRG method is that the difference between  $\mathcal{H}$  on a finite lattice and on an infinite lattice should be negligible along the RG flow. For this to be satisfied, a prerequisite is that the fixed point of the blocking transformation be short ranged. Since this property of the fixed point is to some extent a function of the RG transformation, it is possible to improve results by tuning it. For further discussion on this point, we refer the reader to pp. 570–573 of Ref. 9.

The  $\{K'_{\alpha}\}$  are functions of  $\{K_{\alpha}\}$  and are specified by the RG transformation. Near the fixed point, one can approximate the functional dependence by the linearized transformation matrix  $T_{\alpha\beta}^n$ , which is defined as

$$T_{\alpha\beta}^n = \frac{\partial K'_{\alpha}}{\partial K_{\beta}^{n-1}} = \sum_{\sigma} \frac{\partial K'_{\alpha}}{\partial \langle S_{\sigma}^n \rangle} \frac{\partial \langle S_{\sigma}^n \rangle}{\partial K_{\beta}^{n-1}} . \quad (2.3)$$

Here  $\langle S_{\sigma}^n \rangle$  is the expectation value of the  $\sigma$ th spin operator on the  $n$ th renormalized lattice and  $K_{\beta}^n$  is the corresponding coupling. Since the change in couplings is obtained by keeping only the leading linear term, the method requires that calculations be done close to  $\mathcal{H}^*$  and that  $b$  be small. The two terms on the right-hand side of Eq. (2.3) are connected two-point correlation matrices

$$U_{\sigma\beta}^n \equiv \frac{\partial \langle S_{\sigma}^n \rangle}{\partial K_{\beta}^{n-1}} = \langle S_{\sigma}^n S_{\beta}^{n-1} \rangle - \langle S_{\sigma}^n \rangle \langle S_{\beta}^{n-1} \rangle , \quad (2.4)$$

$$D_{\sigma\alpha}^n \equiv \frac{\partial \langle S_{\sigma}^n \rangle}{\partial K_{\alpha}^n} = \langle S_{\sigma}^n S_{\alpha}^n \rangle - \langle S_{\sigma}^n \rangle \langle S_{\alpha}^n \rangle , \quad (2.5)$$

and hence

$$\mathcal{T} = D^{-1} U . \quad (2.6)$$

From an ensemble of measurements,  $S_{\alpha}^n$ , we construct the correlation functions given in Eqs. (2.4) and (2.5). Then Eq. (2.6) allows us to calculate properties of the RG flow without knowing the renormalized  $\mathcal{H}^n$ . In particular, the critical exponents are obtained from the eigenvalues of  $T_{\alpha\beta}^n$ .

In this study we analyze the systematic errors that arise in MCRG calculations. To establish notation we give a brief introduction to these. The blocked Hamiltonian consists of all possible couplings that fit on a given size lattice even when the starting Hamiltonian is just nearest neighbor:

$$\mathcal{H}_{nn} = K_{nn} S_{nn} , \quad (2.7)$$

where the interaction

$$S_{nn} = \sum_{\langle ij \rangle} s_i s_j \quad (2.8)$$

is the sum over all distinct nearest-neighbor pairs. A basic assumption of the renormalization-group method is that the renormalized couplings  $\{K_\alpha^n\}$  fall off exponentially with distance between the spins and also with the number of spins in a given interaction term. As mentioned earlier, this assumption—that the fixed point is short ranged—is necessary in order to justify why the critical behavior extracted from a finite system is a faithful representation of the bulk critical behavior. To test this assumption in MCRG calculations, the standard practice is to perform simulations on increasingly larger lattices and by measuring more and more interactions on the blocked lattices. In a computer simulation the number of interactions actually evaluated is a small finite subset of all possible interactions; therefore there exist systematic errors known as truncation errors. These arise because (a) the elements of  $D^{-1}$  constructed from a truncated version of  $D$  are not the same as for the infinite matrix and (b) the eigenvalues of  $\mathcal{T}$  constructed from a product of a truncated  $D^{-1}$  and  $U$  [Eq. (2.6)] are different from those obtained from the full matrix. It was shown in Ref. 10 that to leading order these two errors cancel. This fortuitous cancellation is one reason why MCRG works so well. In order to evaluate and control the residual truncation errors, we have calculated all 53 even and 46 odd interactions that fit in either a  $3 \times 3$  square or a  $2 \times 2 \times 2$  cube of spins.

The accuracy of the calculation of the exponents improves when the  $\mathcal{T}_{\alpha\beta}^n$  are evaluated close to the fixed point. If the starting  $\mathcal{H}$  is critical, then this condition can be satisfied by blocking the lattice a sufficient number of times, i.e.,  $\mathcal{H}^n \rightarrow \mathcal{H}^*$  for large  $n$ . In this case the convergence of the eigenvalues is limited by the starting lattice size. On the other hand, if the starting  $\mathcal{H}$  does not lie on the critical surface, then the RG flow is initially toward the fixed point along the irrelevant directions, but away from it along the relevant directions. In the latter case one does not know, *a priori*, the number of RG steps at which the best estimate can be extracted. This lack of convergence in the eigenvalues of  $\mathcal{T}_{\alpha\beta}$  is the second source of systematic errors in a MCRG calculation. In the Appendix we show how this error affects the results and obtain the leading correction term, using which we extrapolate our data along the RG flow to  $\mathcal{H}^*$ .

In addition to the systematic errors due to truncating the number of operators used in the construction of  $\mathcal{T}_{\alpha\beta}$  and the lack of convergence, the third source of systematic errors is finite-size effects. Even if the fixed point  $\mathcal{H}^*$  of the RG transformation is short ranged, the finite size of the lattice will effect the blocked  $\mathcal{H}$ . This effect will be most significant at the higher levels of blocking, precisely where we want to measure  $\mathcal{T}_{\alpha\beta}^n$  to reduce the second systematic error described above. Previous calculations show that for the 3D Ising model this error is significant only when blocking  $8^3$  lattices down to  $4^3$  lattices.<sup>1,2</sup> We verify this result and conclude that when the lattice being blocked is  $16^3$  or larger, finite-size errors are much small-

er than the statistical error.

In 1984 Pawley *et al.*<sup>1</sup> performed a significant MCRG calculation with high statistics. They ran on four lattice sizes  $8^3$ ,  $16^3$ ,  $32^3$ , and  $64^3$  and at three values of the coupling  $K_{\text{NN}} = 0.221\,61$ ,  $0.221\,66$ , and  $0.221\,69$ . They measured seven even and six odd operators in order to construct  $\mathcal{T}_{\alpha\beta}$ . In the analysis they implicitly assumed that hyperscaling  $d\nu = 2 - \alpha$  holds; MCRG calculations do not test hyperscaling. [Also, in order to determine  $\gamma$ , one has to use the ordinary scaling relation  $(2 - \eta)\nu = \gamma$ .] Their best estimate of the nearest-neighbor critical coupling, using the method described in Sec. IV, was  $K_{\text{NN}}^c = 0.221\,654(6)$ . In order to take into account finite-size effects, lack of convergence, and truncation errors, they first made separate extrapolations in each. Even though the three systematic errors were intertwined, they correctly estimated (in light of the present work) that the largest error was due to the small number of operators measured. Using their extrapolated values of  $\nu$  and  $\eta$  obtained at the three values of the coupling, they obtained their final estimates by interpolation to  $K_{\text{NN}} = 0.221\,654$ , and these were  $\nu = 0.629(4)$  and  $\eta = 0.031(5)$ .

In 1989 Blöte *et al.*<sup>2</sup> repeated the calculation of Pawley *et al.* with similar high statistics, on the same size lattices and at  $K_{\text{NN}} = 0.221\,654$ . They calculated 36 even and 21 odd operators and found that this set is sufficient to overcome truncation errors. They also carried out a systematic study of finite-size effects and showed that finite-size errors are significant only at the highest blocking level, i.e.,  $8^3 \rightarrow 4^3$ . Their estimates are  $K_{\text{NN}}^c = 0.221\,652(6)$ ,  $\nu = 0.629(3)$ , and  $\eta = 0.027(5)$ . The results of Blöte *et al.* supercede those in Ref. 1 since they calculate more operators and performed runs closer to  $K_{\text{NN}}^c$ . Therefore we will primarily make comparisons using the results given in Ref. 2.

The principal remaining limitation of MCRG calculations is the lack of convergence of the eigenvalues of  $\mathcal{T}_{\alpha\beta}^n$ . Even for high-statistics simulations carried out on  $64^3$  lattices using a good estimate for  $K_{\text{NN}}^c$ , finite-size errors set in before the eigenvalues of  $\mathcal{T}_{\alpha\beta}^n$  have converged. In this regard our calculations on  $128^3$  lattices (the largest lattice size we could simulate at the time of starting this calculation in 1988) extend previous results and allow us to make more reliable extrapolations.

### III. DETAILS OF THE SIMULATIONS

We have carried out simulations on  $64^3$  and  $128^3$  lattices at each of the two values of coupling:  $K_{\text{NN}} = 0.221\,654$  (best estimate presented in Ref. 1) and  $K_{\text{NN}} = 0.221\,644$ . Most of our update sequence consists of the combination of a single-cluster update algorithm followed by ten Metropolis sweeps. Early runs were performed with 100 Metropolis sweeps only, and a few runs were done with only the cluster update. Measurements are made at the end of each update sequence. The update parameters and statistics accumulated are given in Table I. For the purpose of error analysis, the data have been divided into a bin size of 10 000 measurements. On both lattice sizes  $64^3$  and  $128^3$ , the highest blocked lattice is  $4^3$ ,

TABLE I. Description of lattices used, update parameters, and statistics.

$K_{NN}$	Update characteristics			Statistics
	Lattice	Cluster	Metropolis	
0.221 654	$64^3$	yes	10 hits	100 K
0.221 654	$128^3$	no	100 hits	25.5 K
0.221 654	$128^3$	yes	0 hits	1.5 K
0.221 654	$128^3$	yes	10 hits	113 K
0.221 644	$64^3$	yes	10 hits	100 K
0.221 644	$128^3$	no	100 hits	20 K
0.221 644	$128^3$	yes	10 hits	120 K

and so measurement of observables has been made on 5 (6) levels, labeled 0–4 (0–5), respectively.

The entire calculation was done on a SIMD (single-instruction, multiple-data) parallel computer called the DAP (Distributed Array Processor). This computer consists of  $D \times D$  bit-serial processing elements (PE's) configured as a cyclic two-dimensional grid with nearest-neighbor connectivity. Originally made by ICL with  $D=64$ , the DAP is currently made by AMT with  $D=32$  and 64, called the DAP 510 and DAP 610, respectively. The Ising-model computer simulation is very well suited to such a machine since the spins can be represented as single-bit (logical) variables. In 3D the system of Ising spins on a  $M \times M \times M$  simple-cubic lattice is "crinkle mapped" onto the  $D \times D$  DAP by storing  $N \times N$  pieces of each of  $M$  planes in each PE:  $M \times M \times M = M \times (N \times D) \times (N \times D)$ , with  $N = M/D$ .

For spin update we use, for two reasons, the single-cluster variant of the Swendsen-Wang algorithm developed by Wolff. First, the dynamical critical exponent for the Wolff algorithm is almost a factor of 2 less than that for the Swendsen-Wang algorithm: 0.28(2) versus 0.50(3) in the case of the 3D Ising model.<sup>3</sup> Second, the Wolff algorithm can be implemented more efficiently on a SIMD computer such as the DAP.<sup>11</sup>

The algorithm is implemented as follows: First, we generate bonds between neighboring spins with probability

$$P(\sigma_i, \sigma_j) = \delta_{\sigma_i, \sigma_j} (1 - e^{-2\beta}). \quad (3.1)$$

Like the spins, these bonds are represented by logical variables and their construction is done in parallel. We then choose a random spin and construct the cluster in which it is located using the Allen-Toral-Wall algorithm as discussed by Dewar and Harris.<sup>12</sup> At each step of the fully parallel implementation of this algorithm, a logical variable `i_am_in_the_cluster` is set to `.TRUE.` at the neighboring site if the connecting bond is active and if the test site is already part of the cluster. This process is iterated until the entire cluster is populated. On the DAP all the spins in each generation are evolved simultaneously, thereby furnishing a wavefrontlike parallelism. Unfortunately, the maximum number of processors doing useful work at any time is only of the order of the square root of the total number of processors (see Ref. 11 for a detailed comparison of algorithms).

The 53 even and 46 odd couplings that are contained in

either a  $3 \times 3$  square or a  $2 \times 2 \times 2$  cube are shown in Figs. 1 and 2, respectively. We also indicate the seven even operators used by Pawley *et al.* (labeled  $P1$ – $P7$  in Fig. 1), and the operators in common with Blöte *et al.* are la-

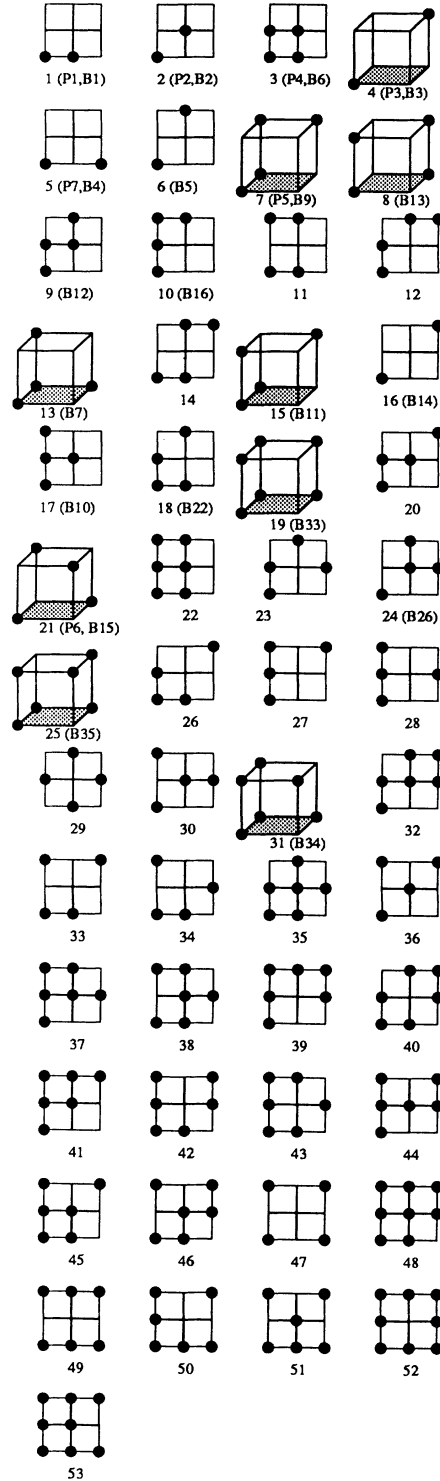


FIG. 1. Fifty-three even operators are shown in the order in which they are used in the MCRG analysis. In parenthesis we show the seven operators used in Ref. 1, marked  $P1$ – $P7$ , and the operators that occur in Ref. 2 labeled with a  $B$ .

beled with a  $B$  followed by a number giving their order as in Ref. 2. The measurement of these interactions is done as follows: We reduce the state of each template of  $3 \times 3$  spins centered about a given spin to a number between  $[0,511]$  and similarly for the  $2^3$  spins to a number between  $[0,255]$ . The sum over the lattice sites and three orientations for the  $3 \times 3$  template is stored as a histogram and similarly for the  $2^3$  template. A simple lookup table then provides a map between these two histograms and the 53 even and 46 odd interactions. The calculation of the state of a  $3 \times 3$  or  $2^3$  block is a homogeneous operation that can be done very efficiently on a vector or a parallel computer.

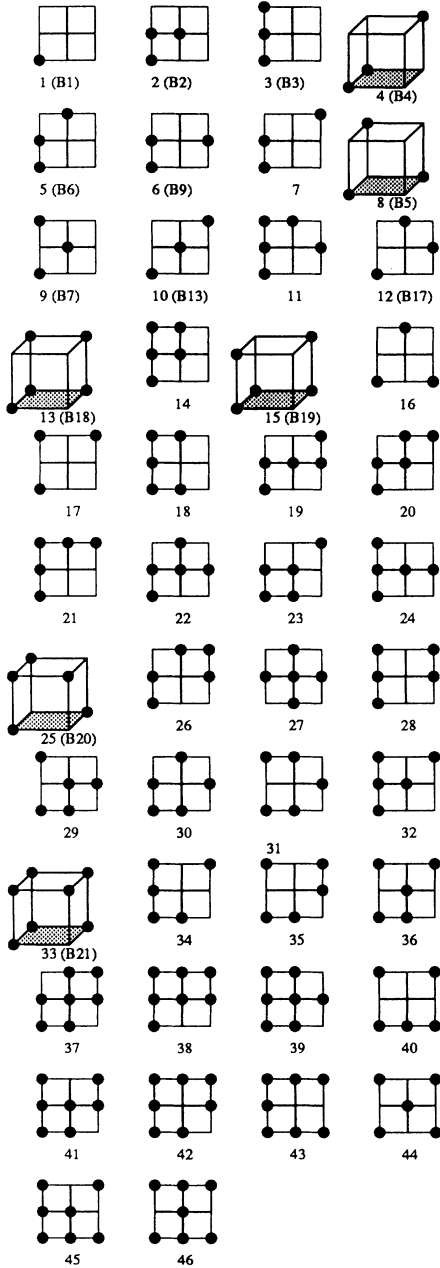


FIG. 2. Forty-six odd operators are shown in the order in which they are used in the MCRG analysis. In parenthesis we show the operators in common with Ref. 2.

The obvious way to make the required histograms is to store one histogram per PE and first do a sum over all the sites resident in its memory. This is very inefficient on the DAP because the PE's lack the hardware functionality to index individually different locations in their respective memories. Also, the memory on a DAP is not sufficient to allow this. Instead, we store a 512-entry histogram in  $D$  pieces along rows of the DAP. Each of these histograms is thus compared as  $D$  columns and  $H$  memory locations, with  $D \times H = 512$ . During the measurement, the  $D$  partial histograms are updated in parallel. The final sum to get the complete histogram is done at the end.

The current implementation of the code requires roughly the same time to do blocking and histogram measurement or one cluster update or 100 Metropolis updates. On a DAP 510, our hybrid update consisting of ten Metropolis plus one cluster update plus blocking and histogram measurement takes on average 127 sec (13.5 sec) for the  $128^3$  ( $64^3$ ) lattices. The DAP 610 is 4 times faster. We estimate that the total time used for this calculation is approximately 11 000 DAP 510 h.

#### IV. NEAREST-NEIGHBOR CRITICAL COUPLING $K_{NN}^c$

To calculate  $K_{NN}^c$  consider two MCRG simulations with the same starting couplings  $K_{NN}$ , but on lattice sizes  $L = b^n = 128$  and  $S = b^{n-1} = 64$ . If  $K_{NN}$  is critical, then under blocking  $H \rightarrow H^*$  and all correlation functions attain their fixed-point values after a sufficient number of blocking steps. For a noncritical starting  $H$ , we can expand about the critical flow in the linear approximation

$$\begin{aligned} \langle L_\alpha^m \rangle - \langle S_\alpha^{m-1} \rangle &= \frac{\partial}{\partial K_{NN}^0} (\langle L_\alpha^m \rangle - \langle S_\alpha^{m-1} \rangle) \Delta K_{NN}^0 \\ &= (\langle L_\alpha^m L_{NN}^0 \rangle_c - \langle S_\alpha^{m-1} S_{NN}^0 \rangle_c) \Delta K_{NN}^0, \end{aligned} \quad (4.1)$$

to determine  $\Delta K_{NN}^0$  for each interaction  $\alpha$ . Note that the expectation values on the left-hand side are calculated on the same size lattices; thus most of the finite-size effects should cancel. The new estimate for the critical coupling is given by

$$K_{NN}^c = K_{NN}^0 - \Delta K_{NN}^0. \quad (4.2)$$

The reliability of this estimate is expected to improve as the starting  $K_{NN}$  is tuned closer to  $K_{NN}^c$ .

We have determined the mean  $\Delta K_{NN}^0$  using the complete data set for the two lattices. To determine errors we carried out a single-elimination jackknife procedure with the  $128^3$  data divided into 14 bins, each with 10 000 measurements, and the  $64^3$  data used as one bin of 100 K. Estimates using different interactions  $\alpha$  are not statistically independent. So the final values and error estimates given in Table II are a simple average over the 53 even interactions since they all provide a consistent estimate. Note that at levels 3–4 and 4–5 the variance over the 53 operators is much smaller than the statistical errors. The errors in data starting from  $K_{NN}^0 = 0.221644$  are consid-

TABLE II. Estimates of  $K_{\text{NN}}^c$  as a function of the blocking level for the two simulations. The quoted errors are in the last two decimal places. The first error is statistical, determined using a single-elimination jackknife procedure with the  $128^3$  data divided into 14 bins of 10-K measurements. (The  $64^3$  data was used as one bin of 100 K.) The second error, which represents a systematic error, is the standard deviation computed from the 53 even interactions.

Levels	$K_{\text{NN}}=0.221\,654\,0$	$K_{\text{NN}}=0.221\,644\,0$
1-2	0.221 607 0±16±121	0.221 604 6±23±127
2-3	0.221 640 6±18±27	0.221 639 4±27±31
3-4	0.221 650 0±21±05	0.221 650 1±31±07
4-5	0.221 651 4±26±02	0.221 651 6±37±11

erably larger, even though the two runs have the same statistics. We believe that this is because the starting point lies farther from  $K_{\text{NN}}^c$ .

We use a weighted mean of the results for the two starting couplings to obtain our present best estimate:

$$K_{\text{NN}}^c = 0.221\,652 \pm 0.000\,003 \pm 0.000\,001, \quad (4.3)$$

where the first error is statistical and the second is our estimate of the lack of convergence error obtained by looking at the difference between results on levels 3-4 and 4-5, as given in Table II. Since the convergence is from below, we have rounded up in the last digit.

We now derive the leading corrections to Eq. (4.1). To simplify the discussion we assume that the calculations are done on infinite lattices and that only two scaling fields contribute. Let  $t$  be the deviation of the starting Hamiltonian from  $\mathcal{H}^*$  along the direction of the relevant field and  $u$  along the irrelevant direction. Then we can write the expectation value for a given interaction  $S$  at  $\mathcal{H}$  as

$$S = S^* + ct + du. \quad (4.4)$$

After  $n$  blocking steps,  $\mathcal{H} \rightarrow \mathcal{H}^n$ , and  $S$  is given by

$$S^n = S^* + c\lambda_t^n t + d\lambda_u^n u. \quad (4.5)$$

Therefore

$$\begin{aligned} S^n - S^{n-1} &= ct\lambda_t^{n-1}(\lambda_t - 1) + du\lambda_u^{n-1}(\lambda_u - 1), \\ &= ct\lambda_t^{n-1}(\lambda_t - 1) \left[ 1 + \frac{du\lambda_u^{n-1}(\lambda_u - 1)}{ct\lambda_t^{n-1}(\lambda_t - 1)} \right], \\ &= t \frac{\partial}{\partial t} (S^n - S^{n-1}) \left[ 1 + A \frac{\lambda_u^{n-1}}{\lambda_t^{n-1}} \right]. \end{aligned} \quad (4.6)$$

TABLE III. Final results for the thermal exponent  $y_t$ . In column 4 we have included results obtained by Blöte *et al.* (Ref. 2) for comparison. In column 5 we give estimates of finite-size corrections when blocking  $8^3$  lattices down to  $4^3$  as explained in the text.

Level	0.221 654 $128^3$	0.221 654 $64^3$	0.221 654 $64^3$ (Ref. 2)	Finite-size corrections	0.221 644 $128^3$	0.221 644 $64^3$
0-1	1.4262(27)	1.4249(26)	1.4240(6)	0.0082(8)	1.4239(22)	1.4219(28)
1-2	1.5087(11)	1.5087(15)	1.5068(5)	0.0082(9)	1.5080(18)	1.5103(26)
2-3	1.5500(22)	1.5471(16)	1.5507(14)	0.0093(17)	1.5497(15)	1.5554(28)
3-4	1.5742(29)	1.5633(92)	1.5603(28)	0.0109(76)	1.5607(40)	1.5742(85)
4-5	1.5760(73)			0.0114	1.5611(94)	

This leading analysis shows that the estimates of  $K_{\text{NN}}^c$  will converge by the geometric factor  $\lambda_u/\lambda_t$  as a function of the blocking level  $n$ . For the 3D Ising model we find that  $\lambda_u/\lambda_t \approx 6$ , and data for  $K_{\text{NN}}^c$  (see Table II) do roughly show convergence by this factor. Consequently, we conclude that the result on level 4-5 has essentially converged and that no extrapolation is necessary.

The numbers given in Table II are in excellent agreement with the results of both Pawley *et al.*<sup>1</sup> and Blöte *et al.*<sup>2</sup> for the case  $L=64$  and  $S=32$ , provided that the comparison is made after the same number of blocking steps. This agreement between three independent calculations is a confirmation of the stability of the MCRG method. Note that these calculations used different update algorithms, different random number generators, and were done on different types of computers.

We find that the two couplings  $K_{\text{NN}}=0.221\,644$  and  $0.221\,654$  lie too close together to make sensible interpolation of the results to  $K_{\text{NN}}=0.221\,652$ . So, in the remainder of the paper, we will quote all final estimates from  $K_{\text{NN}}=0.221\,654$  runs since these lie closer to our estimate of  $K_{\text{NN}}^c$ . The results from  $K_{\text{NN}}=0.221\,644$  runs provide a consistency check.

## V. CORRELATION-LENGTH EXPONENT $\nu$

For the 3D Ising model in zero magnetic field,  $T_{\alpha\beta}^n$  factors into two parts according to whether the interactions are even or odd under  $s_i \rightarrow -s_i$ . The correlation-length exponent  $\nu$  is determined from the leading even eigenvalue  $\lambda_t$  of  $T_{\alpha\beta}^n$ :

$$y_t \equiv \frac{1}{\nu} = \frac{\ln \lambda_t}{\ln b}, \quad (5.1)$$

where  $b=2$  is the scale factor of the transformation used. The errors are calculated using the single-elimination jackknife method with data divided into bins of 10 000 measurements.

We show our final results for  $y_t$  determined using all 53 operators on the various blocking levels for the two lattice sizes and for the two values of the coupling in Table III. To facilitate comparison we also display the final results from Blöte *et al.* on the largest lattice simulated by them. We find that up to levels 2-3 all results for  $y_t$  agree within the statistical errors. At level 3-4 we find evidence for finite-size effects by comparing our  $128^3$  and  $64^3$  lattices results. Thus we confirm, within our statistical accuracy, that finite-size effects lead to systematic er-

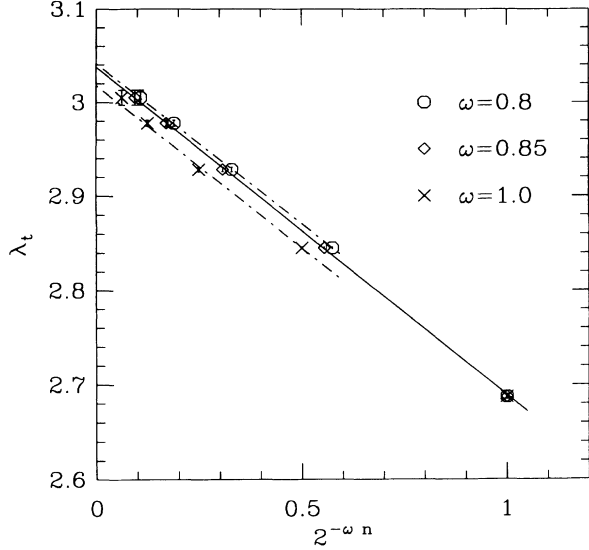


FIG. 3. Extrapolation of  $\lambda_t$  to  $n=\infty$  for three different values of  $\omega$ . Fits with  $\omega=1.0$  and  $0.8$  are made using  $n=1, 2, 3$ , and  $4$  points and all five points for  $\omega=0.85$ . We use different symbols for the same data to help distinguish between the three fits.

rors only on the highest blocking levels (4–5 for  $128^3$  and 3–4 for  $64^3$ ), which corresponds to blocking step  $8^3 \rightarrow 4^3$ .

In order to correct for the finite-size effects in our data on  $128^3$  lattices at level 4–5, we make use of the data of Blöte *et al.* on smaller lattices ( $8^3$ ,  $16^3$ , and  $32^3$ ) as given in Table II of Ref. 2. For example, the correction at level 0–1 is the difference between results after one blocking step on  $64^3$  and  $8^3$  starting lattices. The resulting final estimates for finite-size corrections at  $K_{\text{NN}}=0.221\,654$  and at each of the levels 0–1 to 3–4 are also given in Table III. We use a linear extrapolation of these corrections to estimate the correction at level 4–5. This changes the estimate of  $y_t$  to  $1.5874(73)$ . Note that we do not give an error in the correction term as we do not have a very reliable estimate for it. For the error estimate we simply use the original statistical error.

The final result we are interested in is the value of  $y_t$  at the fixed point. To obtain this we extrapolate  $\lambda_t$  versus the blocking level  $n$  using the relation derived in the Appendix:

$$\lambda_t(n) = \lambda_t^* + a_t b^{-\omega n}, \quad (5.2)$$

TABLE IV. Final results for the exponents after extrapolation to  $n=\infty$  using Eq. (5.2). The data are from the  $K_{\text{NN}}=0.221\,654$  run on  $128^3$  lattices. Our preferred values are ones with  $\omega=0.85$ . For comparison we also give results (marked with an asterisk) obtained using the extrapolation  $y(n)=y^*+b^{-\omega n}$ , as used in Refs. 1 and 2.

$\omega$	$y_t$	$\nu$	$y_h$	$\eta$
1.0	1.594(2)	0.627(1)	2.4842(1)	0.0316(2)
0.85	1.603(1)	0.624(1)	2.4868(1)	0.0262(2)
0.8	1.605(2)	0.623(1)	2.4879(1)	0.0242(3)
1.00*	1.595(3)	0.627(1)	2.4843(3)	0.0314(6)
0.85*	1.606(2)	0.623(1)	2.4869(3)	0.0262(6)
0.80*	1.606(3)	0.622(1)	2.4880(3)	0.0240(6)

where  $\omega$  is the leading correction-to-scaling exponent. The calculation of  $\omega$  is discussed in Sec. VIII and our best estimate is  $\omega=0.8-0.85$ . To show the dependence of  $\lambda_t^*$  on  $\omega$ , we plot the data in Fig. 3 using  $\omega=0.8, 0.85$ , and  $1.0$  and make a linear extrapolation for each. We find that (a) for  $\omega=0.85$  the fit goes through all the data points, (b) for  $\omega=0.80$  we can fit points with  $n=1, 2, 3, 4$ , and (c)  $\omega=1.0$  fit is not good. The final results are shown in Table IV. We find that the spread due to the uncertainty in the value of  $\omega$  used for the extrapolation is comparable to the statistical errors. We take  $\omega=0.85$  as our preferred value based on the quality of the fit. With this choice the final result is

$$y_t^* = 1.603(1) \Rightarrow \nu = 0.624 \pm 0.001 \pm 0.002, \quad (5.3)$$

where the second error is our estimate of the systematic error coming from the uncertainty in  $\omega$ . On comparing this result with the value on  $128^3$  lattices [ $1.5874(73) \Rightarrow \nu=0.630(3)$ ], it is clear that the change due to the extrapolation is much larger than the statistical errors.

In Table IV we also give the results obtained with the extrapolation method used in Refs. 1 and 2 [see Eq. (A9) in the Appendix]. The final central values from the two methods are indistinguishable. We do find that the quality of the fit using Eq. (5.2) i.e., using the eigenvalue data is slightly better. This is reflected by the smaller error estimates.

To investigate the truncation errors we show, in Fig. 4, the convergence of  $y_t$  as a function of the number of operators included in  $T_{\alpha\beta}^n$ . We find that the largest change occurs on adding the two-spin diagonal operator. Thereafter, the convergence is essentially monotonic and from above. In general, the number of operators necessary in order to get a converged value depends on the precise operator order used, as does the rate of convergence. To our knowledge no well-defined method for ordering operators by importance exists, and so we have used an *ad hoc* recipe based on minimizing the number of spins in an interaction and the sum of the distance between them. This is shown in Fig. 1. For this operator order we find that approximately 17 leading operators on level 0–1 and about 27 operators on level 4–5 are necessary. Thereafter, as more operators are added, the variation in the eigenvalue is only about 10% of the statistical

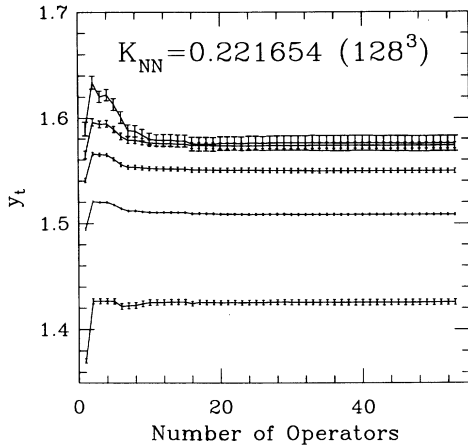


FIG. 4. Convergence of  $y_t$ , as the number of operators is increased in the order shown in Fig. 1. Even though the errors overlap, the data at level 4–5 consistently lies above that at level 3–4.

errors. It is important to note that our final results are obtained using all the operators, and so the precise order plays no role. We plan to investigate in a future calculation the effect of the two leading interactions not measured here, the two-spin operator separated by three sites along an axis and the four-spin operator consisting of four adjoining spins along an axis.

## VI. CORRELATION-FUNCTION EXPONENT $\eta$

The correlation-function exponent  $\eta$  is given by

$$\eta = d + 2 - 2 \frac{\ln \lambda_h}{\ln b} \equiv d + 2 - 2y_h, \quad (6.1)$$

where  $b=2$ ,  $d=3$ , and  $\lambda_h$  is the largest eigenvalue of  $\mathcal{T}_{\alpha\beta}$  constructed from odd interactions. In Table V we show our final results for  $y_h = \ln \lambda_h / \ln b$  and, for comparison, include the results from Blöte *et al.* in column 4. There is very good agreement between results from different calculations on the  $64^3$  lattices at all blocking levels except level 3–4 where the result from Ref. 2 lies  $\sim 3\sigma$  higher. We believe, given the consistency of all the other eigenvalues, that this is most likely due to an underestimate of the statistical errors.

As in the case of  $y_t$ , finite-size effects show up only when blocking  $8^3$  lattices down to  $4^3$ . The finite-size corrections for the first four levels are shown in column 5

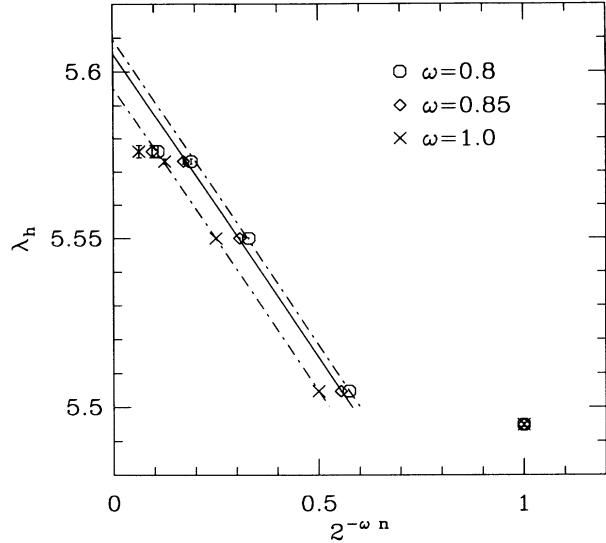


FIG. 5. Extrapolation of  $\lambda_h$  to  $n=\infty$  for three different values of  $\omega$ . The fits are based on blocking levels  $n=1, 2, 3$ , and 4.

of Table V. We use the mean value at the first three levels, 0.00037, as an estimate of the correction on level 4–5. (We exclude the result at level 3–4 in constructing the average because of the large difference between our results on  $64^3$  starting lattices and those given in Ref. 2.) Including this correction shifts our estimate at level 4–5 from 2.47890(107) to 2.47927(107). Just as in the case of  $y_t$ , we cannot reliably estimate the error in the correction, and so we quote only the statistical error.

In Fig. 5 we show fits to  $\lambda_h$  versus  $2^{-\omega n}$  using  $n=1-4$  data. There is no significant difference in the quality of the fit for different values of  $\omega$ , and the value at  $n=4$  is much lower than the fit in all three cases. We believe that this is due to an underestimation of the statistical errors and finite-size corrections. The final results are given in Table IV along with those obtained using the extrapolation procedure of Ref. 1 for comparison. Note that the spread in  $y_h^*$  due to the uncertainty in  $\omega$  is larger than the statistical errors. For our final estimate we quote results with  $\omega=0.85$ :

$$y_h^* = 2.4868(1) \Rightarrow \eta = 0.0262 \pm 0.0002 \pm 0.0030, \quad (6.2)$$

where the second error is an estimate of the systematic error due to the uncertainty in the value of  $\omega$  used in the extrapolation.

TABLE V. Final results for the magnetic exponent  $y_h$ . The rest is the same as in Table III.

Level	0.221 654 128 <sup>3</sup>	0.221 654 64 <sup>3</sup>	0.221 654 64 <sup>3</sup> (Ref. 2)	Finite-size corrections	0.221 644 128 <sup>3</sup>	0.221 644 64 <sup>3</sup>
0–1	2.458 06(34)	2.457 80(48)	2.457 94(11)	0.000 22(13)	2.457 72(30)	2.457 81(28)
1–2	2.460 68(10)	2.460 28(19)	2.460 68(4)	0.000 62(9)	2.460 32(8)	2.460 77(26)
2–3	2.472 51(13)	2.472 10(39)	2.472 43(12)	0.000 28(22)	2.471 95(16)	2.471 56(33)
3–4	2.478 50(45)	2.475 92(105)	2.479 07(64)	0.002 58(114)	2.476 71(41)	2.475 25(180)
4–5	2.478 90(107)			0.000 37	2.474 00(145)	

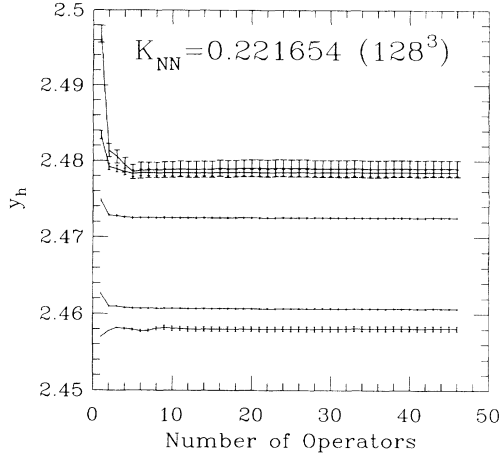


FIG. 6. Convergence of  $y_h$  as the number of operators is increased in the order shown in Fig. 2. Even though the errors overlap, the data at level 4–5 consistently lies above that at level 3–4.

We show the behavior of  $y_h$  as a function of the number of operators included in the construction of  $T_{\alpha\beta}^n$  in Fig. 6. The convergence is faster than that for  $y_t$ , and we find no significant change after including the first 20 operators. Both Figs. 4 and 6 make it clear why it is necessary to concentrate on reducing the statistical errors at the higher blocking levels.

### VII. WILSON'S METHOD FOR EXTRACTING THE LEADING EXPONENTS

Wilson proposed a method to calculate the leading eigenvalues using the flow away from the critical surface.<sup>13</sup> This method does not require the starting coupling to lie on the critical surface and uses the correlation functions directly. Consider the two-point connected correlation function  $\langle S_\alpha^i S_\beta^j \rangle_c$  with the blocking level  $j > i$ . We can expand  $S_\alpha^i$  in terms of the eigenoperators  $O_\alpha^i$  of the RG transformation. Then, to leading order,

$$\begin{aligned} \langle S_\alpha^i S_\beta^j \rangle_c &= \sum_\mu c_{\alpha,\mu}^i \langle O_\mu^i S_\beta^j \rangle_c \\ &= \sum_\mu \lambda_\mu^{j-i} c_{\alpha,\mu}^j \langle O_\mu^j S_\beta^j \rangle_c \\ &\sim \lambda_t^{j-i} c_{\alpha,t}^j \langle O_t^j S_\beta^j \rangle_c, \end{aligned} \quad (7.1)$$

where  $\lambda_t$  is the leading relevant eigenvalue. We assume that close to  $H^*$  the level dependence in  $O_\mu^i$  and in the expansion coefficients  $c_{\alpha,\mu}^i$  can be neglected. Then, for each  $\alpha$  and  $\beta$ , the ratio  $\langle S_\alpha^i S_\beta^j \rangle_c / \langle S_\alpha^{i+1} S_\beta^j \rangle_c$  gives an estimate for the leading eigenvalue  $\lambda_t$ . Corrections to this behavior are suppressed geometrically, as can be seen by assuming that only two scaling fields  $O_t$  and  $O_u$  contribute to the sum. Then

$$\frac{\langle S_\alpha^i S_\beta^j \rangle_c}{\langle S_\alpha^{i+1} S_\beta^j \rangle_c} = \lambda_t \frac{1 + (\lambda_u/\lambda_t)^{j-1} X}{1 + (\lambda_u/\lambda_t)^{j-i-1} X}, \quad (7.2)$$

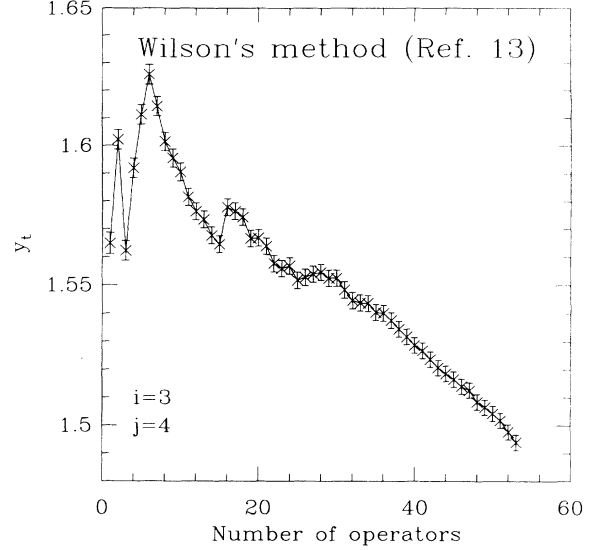


FIG. 7. Behavior of  $y_t$  extracted using Wilson's method as a function of the number of operators used in the analysis. The data are for  $i=3$  and  $j=4$  on the  $128^3$  lattices run at  $K_{NN}=0.221654$ .

where  $X = c_u \langle O_u^i S_\beta^j \rangle_c / c_t \langle O_t^i S_\beta^j \rangle_c$ . Thus the method should improve as  $j-i$  is made large. Also, it should be reliable for models where  $\lambda_u/\lambda_t$  is small and for interactions for which  $X$  is small. Needless to say, one should try to choose the starting  $H$  to lie close to the fixed point.

We show typical results for  $y_t$  and  $y_h$  as a function of the number of operators at levels  $i=3$  and  $j=4$  in Figs. 7 and 8. The data is from  $128^3$  lattices at  $K_{NN}=0.221654$ . The statistical error on each data point is obtained by doing a single-elimination jackknife calculation over the 14 bins. It is clear from these figures that the data do not show any stability with respect to the number of operators. Also, the problem is more severe for the odd sector. Thus a straightforward application of this method does

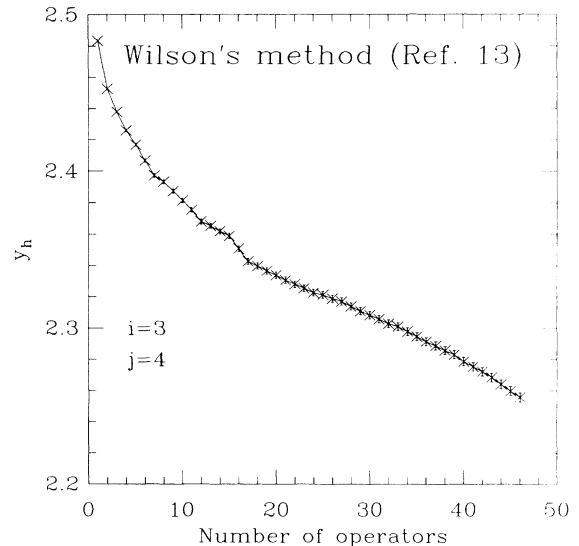


FIG. 8. Same as in Fig. 7, except that the data are for  $y_h$ .

TABLE VI. Results for the thermal exponent  $y_t$ , obtained using Wilson's method. We average over the first 20 operators and quote the variance as the error estimate.

Level $i$	Level $j$	0.221 654 128 <sup>3</sup>	0.221 654 64 <sup>3</sup>	0.221 644 128 <sup>3</sup>	0.221 644 64 <sup>3</sup>
0	1	1.445(068)	1.446(076)	1.443(069)	1.444(077)
0	2	1.442(047)	1.443(050)	1.441(047)	1.441(050)
0	3	1.437(043)	1.437(044)	1.437(043)	1.436(044)
0	4	1.436(042)	1.435(043)	1.435(042)	1.435(042)
0	5	1.435(042)		1.435(042)	
1	2	1.506(054)	1.504(069)	1.504(055)	1.505(070)
1	3	1.503(026)	1.502(032)	1.501(027)	1.503(033)
1	4	1.498(019)	1.496(022)	1.495(020)	1.498(023)
1	5	1.497(018)		1.492(020)	
2	3	1.553(060)	1.539(096)	1.552(059)	1.545(096)
2	4	1.550(024)	1.541(045)	1.550(022)	1.546(044)
2	5	1.544(014)		1.544(011)	
3	4	1.567(090)	1.522(209)	1.559(088)	1.526(206)
3	5	1.569(039)		1.559(038)	

not give reliable results. This is very different from the situation in the 2D model where Wilson's method gives results comparable to those from  $\mathcal{T}_{\alpha\beta}$  (see pp. 564–565 in Ref. 9).

Since we get a similar behavior for all blocking levels, we give in Table VI the value of  $y_t$ , keeping the leading 20 operators in the analysis. The error quoted is the variance over the  $20 \times 20$  correlation functions. We deduce the following qualitative features from the data: The value of  $y_t$  does increase with level  $i$ , and finite-size effects are observable only for  $i = 3$ . Also, the errors decrease as  $j$  is increased for fixed  $i$ . Overall, because of the lack of convergence as a function of the number of interactions included, we do not pursue this method any further in this study.

### VIII. SUBLEADING EXPONENTS AND REDUNDANT OPERATORS

The scaling behavior of the free energy, written as a function of two relevant scaling fields  $t$  and  $h$  and one irrelevant field  $u$ , is

$$\begin{aligned}
 f(t, h, u) &= \left[ \frac{t}{\tau} \right]^{d/y_t} f \left[ \tau, \left[ \frac{\tau}{t} \right]^{y_h/y_t} h, \left[ \frac{\tau}{t} \right]^{y_u/y_t} u \right] \\
 &= \left[ \frac{t}{\tau} \right]^{2-\alpha} f \left[ \tau, \left[ \frac{\tau}{t} \right]^\Delta h, \left[ \frac{\tau}{t} \right]^{-\theta} u \right], \quad (8.1)
 \end{aligned}$$

where  $\tau$  is some reference value of  $t$ . The exponent that characterizes scaling violations in thermodynamic functions is  $y_u/y_t \equiv y_{t,2}/y_t \equiv -\theta$ . For example, the asymptotic expansion for the specific heat is

$$C_v = Ct^{-\alpha}(1 + c_\theta t^\theta + c_1 t + \dots). \quad (8.2)$$

The nonanalytical correction  $c_\theta t^\theta$  is significant when calculations are done away from the fixed point and for  $u \neq 0$ , and so it is important to evaluate it. In a MCRG

calculation this correction-to-scaling exponent is determined from the subleading eigenvalue  $\lambda_{t,2}$  in the even sector:  $\omega \equiv -y_{t,2} = \ln \lambda_{t,2} / \ln b$ . Once  $\omega$  is known, the exponents  $\nu$  and  $\eta$  calculated along a critical RG flow can be extrapolated to the fixed point using Eq. (5.2).

We find that while the statistical errors in leading even eigenvalue  $\lambda_t$  are small, the same is not true of  $\lambda_{t,2}$ . Also, the eigenvalue analysis is not very stable; often the second and third eigenvalues merge into a complex pair when the number of operators is  $\geq 15$ , and in some cases the value fails to converge as more operators are included. For this reason we do not present a detailed analysis of the data and caution the reader that a higher-statistics study is required. The final results are given in Table VII. Our present best estimate is the interval

$$\omega = 0.80 - 0.85 \equiv \theta = 0.5 - 0.53. \quad (8.3)$$

We use  $\omega = 0.85$  as our preferred value for the purpose of extrapolation since it gives a good fit to  $\lambda_t$  data for all  $n$ , as shown in Fig. 3.

In the odd sector the MCRG analysis is very stable. We find that the third eigenvalue is  $\leq 0.3$  and does not mix with the second to form a complex pair. Also, the

TABLE VII. Final results for the correction-to-scaling exponent  $\omega$ . These results have been obtained with the first 20 operators, and the errors were estimated using a single-elimination jackknife method as explained in the text. Entries marked with an asterisk correspond to cases where the eigenvalue analysis was not very stable, as explained in the text.

Level	0.221 654 128 <sup>3</sup>	0.221 654 64 <sup>3</sup>	0.221 644 128 <sup>3</sup>	0.221 644 64 <sup>3</sup>
0–1	0.95(7)*	0.94(9)	0.90(8)	0.86(5)
1–2	0.85(9)	0.80(6)	0.79(5)	0.80(8)
2–3	0.84(7)	0.66(7)*	0.80(5)	0.85(8)
3–4	0.83(7)*	0.45(6)*	0.79(7)*	0.53(8)*
4–5	0.60(5)*		0.42(6)*	

TABLE VIII. Results for the subleading magnetic exponent. These results have been obtained with all 46 odd operators, and the errors are calculated using a single-elimination jackknife method as explained in the text.

Level	0.221 654 128 <sup>3</sup>	0.221 654 64 <sup>3</sup>	0.221 644 128 <sup>3</sup>	0.221 644 64 <sup>3</sup>
0-1	0.091(23)	0.060(33)	0.060(33)	0.091(17)
1-2	0.283(16)	0.278(9)	0.255(19)	0.253(14)
2-3	0.332(11)	0.343(15)	0.324(17)	0.364(19)
3-4	0.398(17)	0.380(20)	0.359(18)	0.415(21)
4-5	0.401(23)		0.380(24)	

second eigenvalue converges on all levels once the first 20 operators are included and the statistical errors are small. The final results for the subleading exponent  $y_{h,2} = \ln \lambda_{h,2} / \ln 2$  are given in Table VIII. Even though the convergence of  $y_{h,2}$  as a function of the blocking level is, as shown in Fig. 9, slow, there can be little doubt that it is relevant. We estimate that

$$y_{h,2} = 0.42 \pm 0.02 \pm 0.02. \quad (8.4)$$

This result is consistent with the value quoted in Ref. 2. Theoretically, there is no motivation for two relevant operators in the odd sector of the 3D Ising model, and this surprising MCRG result needs to be explained.

In Ref. 1 it was conjectured that this subleading eigenvalue corresponds to a redundant operator and therefore does not contribute to measurable thermodynamic quantities. Pawley *et al.* pointed out that the  $\phi^3$  operator in the  $\lambda\phi^4$  theory is redundant; however, they did not have a way of relating it to the Ising interactions. This problem was overcome by Murthy and Shankar who developed a systematic method for calculating redundant operators for Ising models<sup>14</sup> and wrote down a number of redundant operators for both the 2D and 3D Ising models. Unfortunately, these are not derived as a consequence of

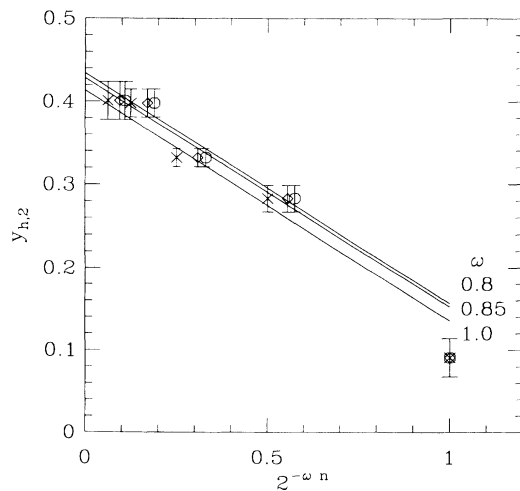


FIG. 9. Extrapolation of  $y_{h,2}$  to  $n = \infty$  for three different values of  $\omega$ . The fits are based on blocking levels  $n = 1, 2, 3,$  and  $4$ .

a RG transformation, and so they are not eigenvectors and are therefore not obviously related to the possible redundant eigenvectors obtained in a MCRG analysis. Using as example the 2D Ising model, Shankar and Gupta<sup>15</sup> were able to develop a strategy to identify redundant operators by making use of the analytical results of Ref. 14. In the following we first review the method and then apply it to show that the subleading odd eigenvector is redundant in 3D.

Consider the situation in which the analytical calculation predicts a redundant operator  $\Omega$  in a subspace of two interactions  $\mathcal{O}_1$  and  $\mathcal{O}_2$ . In this subspace MCRG analysis will give two eigenvectors: one associated with the relevant exponent, thereby forcing the second to be redundant and identical to  $\Omega_1$ . Thus, in this special circumstance where  $\Omega$  lies in a two-dimensional subspace, it is guaranteed to be an eigenvector. If  $\Omega$  lies in a space of three or more operators, then it is not *a priori* an eigenvector and the method loses its predictive power.

We first illustrate this method for the 2D Ising model where it works perfectly. We use the same notation for operator labeling as given in Fig. 2 and replace  $\Omega_i$  by  $\tilde{\Omega}_i$  in order to distinguish from the 3D case. The analytic calculation predicts a redundant operator  $\tilde{\Omega}_1$  in the two-dimensional subspace of  $\mathcal{O}_1$  and  $\mathcal{O}_2$ . The subleading MCRG eigenvector in the same subspace, obtained using the  $2 \times 2$  majority-rule transformation, agrees, within statistical errors, with  $\tilde{\Omega}_1$  and was therefore identified as redundant. In an enlarged space of three interactions, i.e., including  $\mathcal{O}_3$ , Murthy and Shankar had predicted a second redundant operator  $\tilde{\Omega}_2$ . Again, in this restricted subspace, the second and third MCRG eigenvectors have to be redundant; however, now they are only required to be a linear combination of  $\tilde{\Omega}_1$  and  $\tilde{\Omega}_2$  since the  $\tilde{\Omega}_i$  are no longer eigenvectors. Data show that the second MCRG eigenvector is very close to  $\tilde{\Omega}_1$ , as expected by continuity, and that both eigenvectors can be expressed as a linear combination of  $\tilde{\Omega}_1$  and  $\tilde{\Omega}_2$  and a negligible leftover piece. It should not come as a big surprise that the method works so well for the 2D model.

Now we extend the analysis to the 3D model. The redundant operators in the subspace of the first few dominant interactions are predicted to be<sup>14,15</sup>

$$\Omega_1 = \mathcal{O}_1 - 0.174\mathcal{O}_2 + 0.036\mathcal{O}_8 \quad (8.5)$$

and

$$\Omega_2 = \mathcal{O}_1 - 0.116\mathcal{O}_2 - 0.232\mathcal{O}_3 + 0.024\mathcal{O}_9, \quad (8.6)$$

Since the contribution of  $\mathcal{O}_8$  to  $\Omega_1$  is very small, we expect  $\Omega_1$  to almost be a redundant eigenvector in the space spanned by  $\mathcal{O}_1$  and  $\mathcal{O}_2$ . Denoting the MCRG eigenvectors by  $|R_i\rangle_j$ , where the subscript  $i$  denotes that it corresponds to the  $i$ th largest eigenvalue and  $j$  is the dimension of  $\mathcal{T}_{\alpha\beta}$  used in the MCRG analysis, we get

$$|R_2\rangle_2 = \mathcal{O}_1 - 0.156(4)\mathcal{O}_2, \quad (8.7)$$

which is indeed very close to  $\Omega_1$ . The difference is of similar magnitude as the neglected coefficient of  $\mathcal{O}_8$ . This is the best that can be expected of the method in this case. The error quoted in the coefficient of  $\mathcal{O}_2$  includes the variation over levels 0–1 to 4–5 and between the two runs on  $128^3$  lattices. As a technical aside, we point out that even though the redundant eigenoperator does not change significantly along the RG flow, there could be a large effect at the first blocking step which we have no way of evaluating. This could also contribute to the difference between  $|R_2\rangle_2$  and  $\Omega_1$  since the  $\Omega_i$  are calculated at the nearest-neighbor coupling  $K_{\text{NN}} = 0.221654$ .

Having identified the redundant operator in the two-dimensional space, we can trace how it changes as we extend the MCRG analysis to include the five interactions present in  $\Omega_1$  and  $\Omega_2$ . The eigenvector corresponding to the same subleading eigenvalue is

$$\begin{aligned} |R_2\rangle_3 &= \mathcal{O}_1 - 0.12\mathcal{O}_2 - 0.06\mathcal{O}_8, \\ |R_2\rangle_4 &= \mathcal{O}_1 - 0.12\mathcal{O}_2 - 0.03\mathcal{O}_3 - 0.06\mathcal{O}_8, \\ |R_2\rangle_4 &= \mathcal{O}_1 - 0.13\mathcal{O}_2 - 0.08\mathcal{O}_3 - 0.03\mathcal{O}_9, \\ |R_2\rangle_5 &= \mathcal{O}_1 - 0.12\mathcal{O}_2 - 0.02\mathcal{O}_3 - 0.05\mathcal{O}_8 \\ &\quad - 0.01\mathcal{O}_9, \end{aligned} \quad (8.8)$$

where we have rounded all coefficients to two decimal places. In this expanded space of interactions, we cannot make an identification between analytic and numerical results since the  $\Omega_i$  are neither eigenvectors nor linearly independent. Said in a different way, even though the dimensionality of the space of redundant operators is constant near  $\mathcal{H}^*$ , their explicit form depends on the method used to generate them.

To summarize, the method we use to confirm that an eigenvector  $|R\rangle$  is redundant works well only when the corresponding  $\Omega$  is an eigenvector. This condition is automatically satisfied if the  $\Omega$  lies in a two-dimensional subspace of interactions. We show that this is almost the case for the 3D model. In a larger space of interactions the method, in general, fails because the  $\Omega_i$  are no longer eigenvectors. So, unless there is a fortuitous agreement between the  $|R_i\rangle$  and the  $\Omega_j$ , as in the case of the 2D Ising model where we could identify two redundant operators in the subspace of three short range interactions, it is difficult to identify redundant operators by requiring an agreement between numerical and analytical results. One simple procedure that will further confirm that  $|R_2\rangle$  is redundant is to repeat the calculation with a different blocking transformation and check whether the corre-

sponding subleading eigenvalue changes in magnitude.

Redundant operators can obscure MCRG results in two ways: (a) If they are relevant, then  $\mathcal{H}^n$  does not converge under repeated RG transformations (the expectation values  $\langle S_\alpha \rangle$  continue to change subject to the constraints imposed by the redundant operators), and (b) they can interfere with the identification of the universal scaling exponents. Fortunately, neither possibility is a problem in the 3D Ising model. First, the presence of a relevant redundant operator in the odd sector is benign because the fixed point is at zero odd couplings, and this property is preserved under MCRG. Second, Murthy and Shankar did not find a redundant operator in the even sector which could be written in terms of the first few interactions given in Fig. 1. Redundant operators, if present in the even sector, are therefore expected to be suppressed as they would be associated with very small eigenvalues. Thus we believe that the subleading eigenvector in the even sector is physical and is responsible for corrections to scaling; i.e., it is sensible to identify it with the exponent  $\omega$ . (We have no way of testing whether the poor signal seen when extracting  $\lambda_{i,2}$  is due to interference with a redundant operator.) Finally, the large difference between the leading and subleading eigenvalues in both the even and odd sectors suggests that the analysis given in the Appendix for extrapolation of the relevant eigenvalues to  $\mathcal{H}^*$  is reliable.

## IX. COMPARISON OF MCRG RESULTS WITH THOSE FROM OTHER METHODS

Since its inception in 1920, the Ising model has been a test bed for most analytical and numerical techniques in statistical mechanics. To facilitate comparison with our results, we list the popular methods and their predictions for the critical properties  $K_{\text{NN}}^c$ ,  $\eta$ ,  $\gamma$ , and  $\nu$ .

Le Guillou and Zinn-Justin<sup>16</sup> have carried out a series analysis using the fifth-order  $\epsilon$  expansion for the critical exponents. They find stable results for  $2 \leq D \leq 4$  dimensions, and their results are within errors equal to the exact values at  $D=2$ . So they modify their analysis to incorporate the exact results for the 2D Ising model. With this correction their present estimates are  $\gamma = 1.2390(25)$ ,  $\nu = 0.6310(15)$ ,  $\beta = 0.3270(15)$ , and  $\eta = 0.0375(25)$ .

A great deal of work has been done to extract exponents using series analysis of thermodynamic quantities such as the specific heat, magnetization, magnetic susceptibility, etc., and their derivatives. Recently, this technique has been improved by incorporating nonanalytic confluent corrections to the leading scaling behavior [for example, see Eq. (8.2)] and by the use of biased inhomogeneous differential approximants. Including nonanalytic corrections changed the estimate of exponents to the point where there is no obvious evidence of hyperscaling violations. Thus, in the analysis reviewed below, it is tacitly assumed that there are no hyperscaling violations.

Adler<sup>17</sup> has analyzed the series for susceptibility on lattices with different coordination numbers. For the simple-cubic lattice, she finds that the critical coupling lies in the range  $0.22165 < K_{\text{NN}}^c < 0.22166$ . The estimate of systematic error grows to approximately 3 in the last

TABLE IX. Comparison of critical properties determined from various methods. Values marked with an asterisk were used as an input to calculations. Column 6 gives the values of  $\eta$  obtained using the scaling relation  $\eta=2-\gamma/\nu$ . The labels used to denote the different calculations are the following:  $M_1$ , this work;  $M_2$ , Blöte *et al.* (Ref. 2);  $M_3$ , Pawley *et al.* (Ref. 1);  $E$ , Le Guillou and Zinn-Justin (Ref. 16);  $S_1$ , Adler (Ref. 17);  $S_2$ , Guttman (Ref. 18);  $S_3$ , Guttman (Ref. 19);  $S_4, S_5, S_6$ , Liu and Fisher (Ref. 20);  $S_7$ , Nickel and Rehr (Ref. 21);  $F$ , Ferrenberg and Landau (Ref. 26);  $Z_1$ , Bhanot *et al.* (Ref. 28);  $Z_2$ , Alves, Berg, and Villanova (Ref. 29);  $A$ , Alves, Berg, and Villanova (Ref. 29);  $T$ , Novotny, (Ref. 30).

Method	$K_{NN}^c$	$\nu$	$\eta$	$\gamma$	$\eta=2-\gamma/\nu$
MCRG ( $M_1$ )	0.221 652(3)	0.624(2)	0.026(3)		
MCRG ( $M_2$ )	0.221 652(6)	0.629(3)	0.027(5)		
MCRG ( $M_3$ )	0.221 654(6)	0.629(4)	0.031(5)		
$\epsilon$ expansion ( $E$ )	0.221 530*	0.6310(15)	0.0375(25)	1.2390(25)	
Series analysis ( $S_1$ )	0.221 655(5)	0.631(4)		1.239(3)	0.036(13)
Series analysis ( $S_2$ )	0.221 652*	0.630(2)		1.240(6)	0.032(11)
Series analysis ( $S_3$ )	0.221 657(7)	0.632(3)		1.239(3)	0.040(10)
Series analysis ( $S_4$ )	0.221 630(9)	0.6335(10)		1.2395*	0.043(3)
Series analysis ( $S_5$ )	0.221 692(9)	0.6390(10)		1.250*	0.044(3)
Series analysis ( $S_6$ )	0.221 620(19)	0.6325(5)		1.237*	0.044(2)
Series analysis ( $S_7$ )	0.221 615*	0.6300(15)		1.237(2)	0.037(6)
Finite-size scaling ( $F$ )	0.221 6595(26)	0.6289(8)		1.239(7)	0.030(11)
Zeros of partition function ( $Z_1$ )	0.221 654*	0.6295(10)			
Zeros of partition function ( $Z_2$ )	0.221 654*	0.6285(19)			
Scaling of mass gap ( $A$ )	0.221 57(3)	0.6321(19)			
Transfer matrix ( $T$ )	0.220 570	0.6302			

place at the ends of the interval. The estimate for exponents is  $\gamma=1.239(3)$  and  $\nu=0.631(4)$ .

Guttman<sup>18</sup> initially estimated  $\gamma=1.240(6)$  and  $\nu=0.630(2)$  from series analysis for the zero-field susceptibility and its second derivative with respect to the magnetic field. He used as an input  $K_{NN}^c=0.221\,652$ . Later, he reexamined the series using the method of integral approximants<sup>19</sup> to obtain  $K_{NN}^c=0.221\,657(7)$ ,  $\gamma=1.239(3)$ , and  $\nu=0.632(3)$ .

Liu and Fisher<sup>20</sup> have reanalyzed the available series using modern extrapolation techniques and exponent estimates. While their main goal was to calculate amplitudes and amplitude ratios, they also provide results for  $K_{NN}^c$  and  $\nu$ . Using as input their favored value  $\gamma=1.2395$ , they find  $K_{NN}^c=0.221\,630(9)$  and  $\nu=0.6335(10)$ .

Nickel and Rehr<sup>21</sup> analyzed the 21-term high-temperature series for the magnetic susceptibility and correlation length on a bcc lattice. They estimate  $\gamma=1.237(2)$  and  $\nu=0.6300(15)$ .

A detailed finite-size scaling study was performed by Barber *et al.*<sup>22</sup> Their results,  $K_{NN}^c=0.221\,650(5)$  and  $\gamma/\nu=1.98(2)$ , have been cast into doubt by Parisi and Rapuano,<sup>23</sup> by Hoogland, Compagner, and Blöte,<sup>24</sup> and by Bhanot, Duke, and Salvador.<sup>25</sup> The presumed culprit is the random-number generator in their specially constructed "Ising-model processor." The calculation by Bhanot, Duke, and Salvador on up to  $44^3$  lattices provides an estimate  $\gamma/\nu=1.964(3)$ .

Recently, Ferrenberg and Landau<sup>26</sup> carried out a high-resolution finite-size scaling analysis using up to  $96^3$  lattices. They incorporated the histogram techniques of Ferrenberg and Swendsen<sup>27</sup> to obtain  $K_{NN}^c=0.221\,6595(26)$ ,  $\nu=0.6289(8)$ , and  $\gamma=1.239(7)$  [from  $\gamma/\nu=1.970(11)$ ].

Another method for analyzing the critical behavior is

to determine numerically the partition function and investigate the finite-size scaling of the complex zeros closest to the real temperature axis. This was first done by Bhanot *et al.*,<sup>28</sup> yielding the estimate  $\nu=0.6295(10)$ . Alves, Berg, and Villanova repeated this calculation,<sup>29</sup> giving  $\nu=0.6285(19)$ ; they also carried out a finite-size scaling analysis of the mass gap in order to extract a second estimate of  $\nu=0.6321(19)$  as well as  $K_{NN}^c=0.221\,57(3)$ . Combining their two estimates for  $\nu$  yields  $0.6303(14)$ .

Finally, Novotny<sup>30</sup> has used a numerical transfer-matrix method to calculate  $K_{NN}^c$  and  $\nu$ . His best estimate is obtained by comparing a  $4\times 4$  with a  $5\times 5$  system. His data show that the convergence of  $K_{NN}^c$  is slow and the present value  $K_{NN}^c=0.220\,570$  is far from our results. The value of  $\nu$  converges from below as the system size is increased (in agreement with the behavior of the 2D model); however, it is not yet clear whether the system size is large enough to guarantee monotonic convergence. Otherwise, his estimate,  $\nu=0.6302$ , would provide a lower bound and rule out our result. Unfortunately, it does not seem possible to simulate a  $6\times 6$  system on present computers.

These results are summarized in Table IX and displayed graphically in Figs. 10 and 11. The notation used to label different calculations is given in the caption of Table IX. There is a considerable spread in estimates from different methods. In order to evaluate which method is most reliable and will provide the best answers in the future, it is useful to understand the strengths and weaknesses of the different methods.

The MCRG method has the advantage that each of the four quantities  $K_{NN}^c$ ,  $\nu$ ,  $\eta$ , and  $\omega$  is calculated independently, albeit using the same data. The three sources of systematic errors we have discussed can be reduced

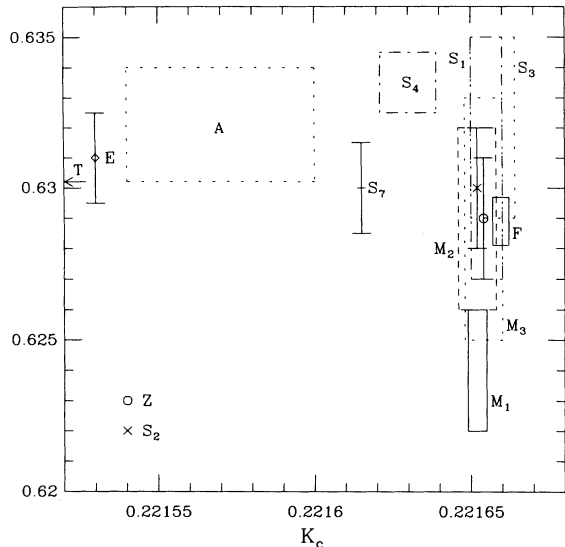


FIG. 10. Spread of results from different methods in the  $K_{NN}, \nu$  plane. The key used to label results from different calculations is given in Table IX. The symbols used for data points  $Z$  (which is the mean of  $Z_1$  and  $Z_2$ ) and  $S_2$  are defined in the lower left corner. The result from Ref. 30 is indicated by an arrow at  $K_{NN}=0.22152$ .

significantly by brute-force computer power. The disadvantage of the method is that it is statistical and that the simulations, done using an estimate for the critical coupling, suffer from critical slowing down. Even though a statistical analysis of  $\mathcal{T}_{\alpha\beta}^n$  shows a remarkable cancellation of errors for the leading even and odd eigenvalues, the largest uncertainty now comes from the extrapolation to  $\mathcal{H}^*$ . In order to do this reliably, we certainly need to improve the estimates for  $\omega$  and  $K_{NN}^c$ .

The advantage of the series analysis is that there are no

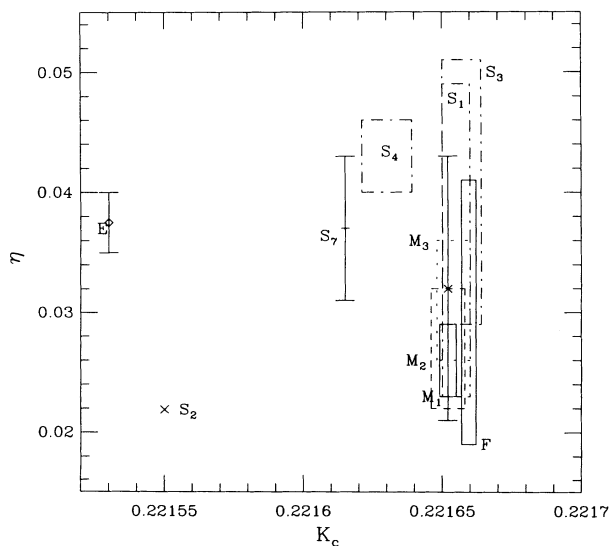


FIG. 11. Spread of results from different methods in the  $K_{NN}, \eta$  plane. The data point  $S_2$  is plotted using the symbol  $\times$  as defined in the lower left corner.

statistical or finite-size errors. However, to extract the four quantities  $K_{NN}^c$ ,  $\nu$ ,  $\gamma$ , and  $\theta$  from series expansions for the susceptibility and correlation length ideally requires a simultaneous fit to two equations similar to Eq. (8.2). Such fits involve at least *eight* free parameters as there are the four additional unknown amplitudes. The present series are not long enough to allow such a fit without getting very large error estimates. Furthermore, as these parameters are highly correlated, a realistic error estimate is near impossible. Even in the existing analysis (where fits are made to a single thermodynamic quantity), the error estimates do not fully take into account the correlations. In addition to the question of estimating errors reliably due to correlations in the parameters, different methods of series analysis give results with a spread that is larger than the quoted errors as is evident from Table IX. Thus it is not obvious to us that our MCRG result  $\nu=0.624(2)$ , which lies about  $(2-3)\sigma$  below results from other methods, is incompatible.

## X. CONCLUSIONS AND FUTURE OUTLOOK

A basic input in numerical and analytical studies is the value of the critical coupling. Our estimate  $K_{NN}^c=0.221652(3)$  is in perfect agreement with previous MCRG studies (we have reduced the error estimate by a factor of 2). The spread in  $K_{NN}^c$ , determined from or used in methods such as series analysis, is very large compared with our errors. The largest clumping of data is around the MCRG values, i.e., between 0.22165 and 0.22166. It would be interesting to repeat the various series analysis fixing  $K_{NN}^c=0.221652$  to see if the estimates for exponents come closer together.

We find that the subleading odd eigenvalue is redundant. Since Monte Carlo simulation are done at zero magnetic field and MCRG does not generate odd couplings, this redundant but relevant operator does not give rise to any complications. On the other hand, the subleading even eigenvector is physical and controls scaling violations.

An accurate measurement of the correction-to-scaling exponent  $\omega$  is essential in order to extract the values of  $\nu$  and  $\eta$  at the fixed point. We find that the statistical quality of the results for  $\omega$  is far less reliable than for  $\gamma$ , and our best estimate consists of the interval 0.8–0.85. The corresponding value  $\theta=0.5-0.53$  is in good agreement with series and RG analysis.<sup>16,17,20,31</sup>

The difference between our result ( $\nu=0.624 \pm 0.001 \pm 0.002$ ) and previous MCRG studies (Refs. 1 and 2) is due to the extrapolation. We have an additional point from the  $128^3$  lattices, and we extrapolate data using our preferred value  $\omega=0.85$ . Our result is  $(2-3)\sigma$  lower than most series,  $\epsilon$  expansion, and finite-size scaling analyses. We believe that this difference is statistically significant.

There is very good agreement in the result for  $\eta$  between our calculation and the value given in Ref. 2. The small difference is due to our use of  $\omega=0.85$  in the extrapolation. In most other methods  $\eta$  is not measured directly, but evaluated using the ordinary scaling relation  $\eta=2-\gamma/\nu$ . Because the value of  $\eta$  is so small, the seem-

ing large difference between results can arise from  $(1-2)\sigma$  errors in  $\gamma$  and  $\nu$ . Using the same scaling relation we get  $\gamma=1.232(4)$ , which is considerably smaller than other estimates.

MCRG calculations give us very accurate values for the three critical parameters  $K_{\text{NN}}^c$ ,  $\eta$ , and  $\nu$  and a reasonable estimate for  $\omega$ . Each parameter is extracted independently and directly from the data. We have shown that the three sources of systematic errors inherent in MCRG calculations can be systematically reduced, and in fact the truncation and finite size errors at all but the highest blocking level have been reduced to far below statistical errors. Future high-statistics simulations on  $256^3$  lattices will significantly reduce the remaining errors and allow us to determine the exponents very accurately.

One serious limitation of the MCRG method is the implicit assumption of hyperscaling. To overcome it requires that we directly measure the renormalized coupling  $g_R$  using thermodynamic functions as proposed by Freedman and Baker<sup>32</sup> and study its scaling properties. We propose to do this calculation as part of a further MCRG study using lattices of size  $64^3$ ,  $128^3$ , and  $256^3$ .

#### ACKNOWLEDGMENTS

We acknowledge useful discussions with H. Blöte, A. Guttmann, M. Novotny, R. Swendsen, and D. Wallace. In particular, we thank R. Shankar for many long discussions on the subject of redundant operators. The authors are grateful to Argonne National Laboratory for providing use of the DAP at the Advanced Computing Research Facility in the Mathematics and Computer Science Division. We also acknowledge the support of the Physics Department at the University of Edinburgh and AMT for the use of their DAP's. We thank G. C. Fox, D. Levine, and P. Messina for their support of this project, James Vernon for running the computer codes at AMT, and K. Barish for participation in early stages of the project. The research of C.F.B. is partly supported by DOE Grant Nos. DE-FG03-85ER25009, DE-AC03-81ER40050, and DE-AC02-86ER40253, and by AFOSR Grant No. AFOSR-89-0422.

#### APPENDIX A: CORRECTIONS TO THE RELEVANT EXPONENTS ALONG THE RG FLOW

We derive the leading correction to the eigenvalues  $\lambda_t$  and  $\lambda_h$  arising from the fact that the simulations are not done at  $\mathcal{H}^*$ . For simplicity we assume that calculations are done on infinite lattices and that only two scaling fields contribute. Let  $K_1=t$  be the deviation of the starting Hamiltonian from  $\mathcal{H}^*$  along the direction of the relevant field and  $K_2=u$  along the irrelevant direction in the even sector of  $\mathcal{T}_{\alpha\beta}^n$ . The expectation value for the two interactions  $S_1$  and  $S_2$  at  $\mathcal{H}$  can be written as

$$\begin{aligned} S_1 &= S_1^* + c_1 t + d_1 u, \\ S_2 &= S_2^* + c_2 t + d_2 u. \end{aligned} \quad (\text{A1})$$

After one blocking step,  $\mathcal{H} \rightarrow \mathcal{H}^1$ ; i.e.,  $K_1^1 = \lambda_t t$ ,

$K_2^1 = \lambda_u u$ , and the  $S_\alpha^1$  are

$$\begin{aligned} S_1^1 &= S_1^* + c_1 \lambda_t t + d_1 \lambda_u u, \\ S_2^1 &= S_2^* + c_2 \lambda_t t + d_2 \lambda_u u. \end{aligned} \quad (\text{A2})$$

From these relations we can construct the matrix  $\mathcal{T}_{\alpha\beta}^1$  using Eq. (2.3):

$$\mathcal{T}_{\alpha\beta}^1 = \begin{pmatrix} \lambda_t & X \lambda_u \\ Y \lambda_t & \lambda_u \end{pmatrix}, \quad (\text{A3})$$

where the explicit form of  $X$  and  $Y$  is not important other than that they vanish for  $u \rightarrow 0$ . The nondiagonal elements of  $\mathcal{T}_{\alpha\beta}$  modify the leading eigenvalue to

$$\lambda_t + A \lambda_u. \quad (\text{A4})$$

This simplified analysis shows how a correction to  $\lambda_t$  arises due to a nonzero value of the irrelevant field  $u$ . Note that this result applies to  $\mathcal{T}_{\alpha\beta}^1$  calculated some distance  $u$  away from  $\mathcal{H}^*$ . To take into account the RG flow under blocking, we now use the simplest form for  $A$  consistent with the requirement that  $A \rightarrow 0$  as  $u \rightarrow 0$ , i.e.,  $A \equiv A(u) \sim au + \dots$ . With this ansatz the leading eigenvalue of  $\mathcal{T}_{\alpha\beta}^{n+1}$  after  $(n+1)$  blocking steps is approximately

$$\lambda_t + (a \lambda_u^n) \lambda_u. \quad (\text{A5})$$

This leading-order estimate allows us to extrapolate the eigenvalue measured along a RG flow to  $\mathcal{H}^*$ . If the measured value at the  $n$ th blocking step is  $\lambda_t(n)$ , then it related to  $\lambda_t^*$  as

$$\lambda_t(n) = \lambda_t^* + a_t \lambda_u^n. \quad (\text{A6})$$

In a MCRG calculation,  $\lambda_u = b^{-\omega}$ , where  $\omega$  is the correction-to-scaling exponent.

A similar analysis for the odd sector shows that the eigenvalue at the  $(n+1)$ th blocking level is

$$\lambda_h + (a \lambda_u^n) \lambda_{h,2}. \quad (\text{A7})$$

Note that along the RG flow only  $\lambda_u$  enters because, in the odd sector, all odd-spin couplings are explicitly set to zero in the simulation and thereafter not generated by the RG procedure. So, once again, we can extrapolate the data using

$$\lambda_h(n) = \lambda_h^* + a_h \lambda_u^n. \quad (\text{A8})$$

We find that the data point at blocking step 0–1 does not conform to this proposed behavior, presumably as a result of the transients.

In Sec. V and VI we extrapolated the data using Eqs. (A6) and (A8). We showed that the data *a posteriori* justify the leading-order analysis. Note that in Refs. 1 and 2 similar expressions were used for the extrapolation, but with, for example,  $\lambda_t$  substituted by  $y_t$ :

$$y_t(n) = y_t^* + c_t b^{-\omega n}. \quad (\text{A9})$$

We discuss the difference between using Eq. (A6) versus Eq. (A9) in the text.

- <sup>1</sup>G. S. Pawley, R. H. Swendsen, D. J. Wallace, and K. G. Wilson, *Phys. Rev. B* **29**, 4030 (1984).
- <sup>2</sup>H. W. J. Blöte, A. Compagner, J. H. Croockewit, Y. T. J. C. Fonk, J. R. Heringa, A. Hoogland, T. S. Smit, and A. L. van Willigen, *Physica A* **161**, 1 (1989).
- <sup>3</sup>U. Wolff, *Phys. Lett. B* **228**, 379 (1989).
- <sup>4</sup>K. Binder, in *Monte Carlo Methods in Statistical Physics*, edited by K. Binder (Springer-Verlag, Berlin, 1979), Vol. 7.
- <sup>5</sup>K. G. Wilson, *Rev. Mod. Phys.* **47**, 773 (1975); Th. Niemeijer and J. M. J. van Leeuwen, in *Phase Transitions and Critical Phenomena*, edited by C. Domb and M. S. Green (Academic, New York, 1976), Vol. 6.
- <sup>6</sup>S.-K. Ma, *Phys. Rev. Lett.* **37**, 461 (1976); L. P. Kadanoff, *Rev. Mod. Phys.* **49**, 267 (1977).
- <sup>7</sup>K. G. Wilson, in *Recent Developments in Gauge Theories, Cargèse 1979*, edited by G. 't Hooft (Plenum, New York, 1980); R. H. Swendsen, *Phys. Rev. Lett.* **42**, 859 (1979).
- <sup>8</sup>K. G. Wilson and J. B. Kogut, *Phys. Rep. C* **12**, 76 (1974); R. H. Swendsen, in *Real Space Renormalization*, Vol. 30 of *Topics in Current Physics*, edited by Th. W. Burkhardt and J. M. J. van Leeuwen (Springer, Berlin, 1982), p. 57.
- <sup>9</sup>R. Gupta, in *Lattice Gauge Theory Using Parallel Processors*, Vol. 1 of CCAST Symposium Proceedings, edited by X. Li, Z. Qiu, and H. Ren (Gordon and Breach, New York, 1987), p. 558.
- <sup>10</sup>R. Shankar, *Phys. Rev. B* **33**, 6515 (1986); R. Gupta, in *Proceedings of the International Conference on Lattice Gauge Theories, Wuppertal, Germany, 1985*, edited by K.-H. Mütter and K. Schilling (Plenum, New York, 1986); *J. Appl. Phys.* **61**, 3605 (1987).
- <sup>11</sup>C. F. Baillie and P. D. Coddington, *Concurrency: Practice and Experience* **3**, 129 (1991).
- <sup>12</sup>R. Dewar and C. K. Harris, *J. Phys. A* **20**, 985 (1987); M. P. Allen (unpublished); R. Toral and C. Wall (unpublished).
- <sup>13</sup>K. G. Wilson, in *Progress in Gauge Field Theory, Cargèse 83*, edited by G. 't Hooft *et al.* (Plenum, New York, 1984), p. 589.
- <sup>14</sup>G. Murthy and R. Shankar, *Phys. Rev. B* **32**, 5851 (1985).
- <sup>15</sup>R. Shankar and R. Gupta, *Phys. Rev. B* **32**, 6084 (1985).
- <sup>16</sup>J. C. Le Guillou and J. Zinn-Justin, *J. Phys. (Paris)* **48**, 19 (1987).
- <sup>17</sup>J. Adler, *J. Phys. A* **16**, 3585 (1983).
- <sup>18</sup>A. J. Guttmann, *Phys. Rev. B* **33**, 5089 (1986).
- <sup>19</sup>A. J. Guttmann, *J. Phys. A* **20**, 1855 (1987).
- <sup>20</sup>A. J. Liu and M. E. Fisher, *Physica A* **156**, 35 (1989).
- <sup>21</sup>B. G. Nickel and J. J. Rehr, *J. Stat. Phys.* **61**, 1 (1990).
- <sup>22</sup>M. N. Barber, R. B. Pearson, D. Toussaint, and J. L. Richardson, *Phys. Rev. B* **32**, 1720 (1985).
- <sup>23</sup>G. Parisi and F. Rapuano, *Phys. Lett.* **157B**, 301 (1985).
- <sup>24</sup>A. Hoogland, A. Compagner, and H. W. J. Blöte, *Physica A* **132**, 593 (1985).
- <sup>25</sup>G. Bhanot, D. Duke, and R. Salvador, *Phys. Rev. B* **33**, 7841 (1986).
- <sup>26</sup>A. M. Ferrenberg and D. P. Landau, *Phys. Rev. B* **44**, 5081 (1991).
- <sup>27</sup>A. M. Ferrenberg and R. H. Swendsen, *Phys. Rev. Lett.* **61**, 2635 (1988).
- <sup>28</sup>G. Bhanot, R. Salvador, S. Black, and R. Toral, *Phys. Rev. Lett.* **59**, 803 (1987).
- <sup>29</sup>N. A. Alves, B. A. Berg, and R. Villanova, *Phys. Rev. B* **41**, 383 (1990).
- <sup>30</sup>M. A. Novotny, in *Transfer Matrix Study of  $d \geq 3$  Ising Models*, International Symposium "Lattice 90," Proceedings of the International Conference on Lattice Field Theory, Tallahassee, Florida, 1990, edited by U. M. Heller *et al.* [*Nucl. Phys. B (Proc. Suppl.)* **20**, 122 (1991)].
- <sup>31</sup>J. Chen, M. Fisher, and B. Nickel, *Phys. Rev. Lett.* **48**, 630 (1982).
- <sup>32</sup>B. A. Freedman and G. A. Baker, *J. Phys. A* **15**, L715 (1982).

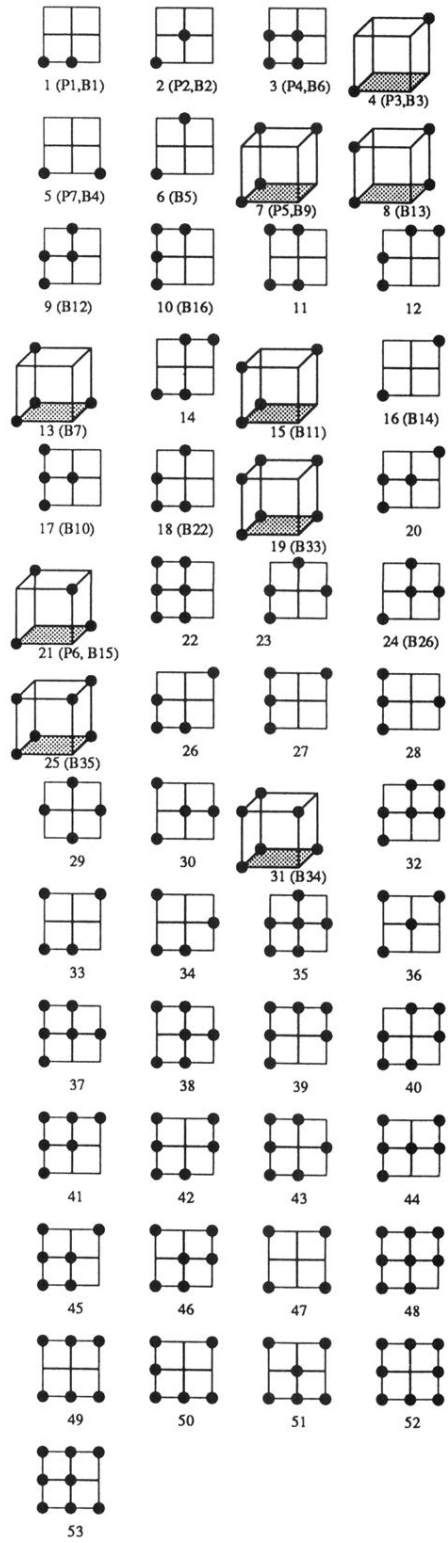


FIG. 1. Fifty-three even operators are shown in the order in which they are used in the MCRG analysis. In parenthesis we show the seven operators used in Ref. 1, marked  $P1-P7$ , and the operators that occur in Ref. 2 labeled with a  $B$ .

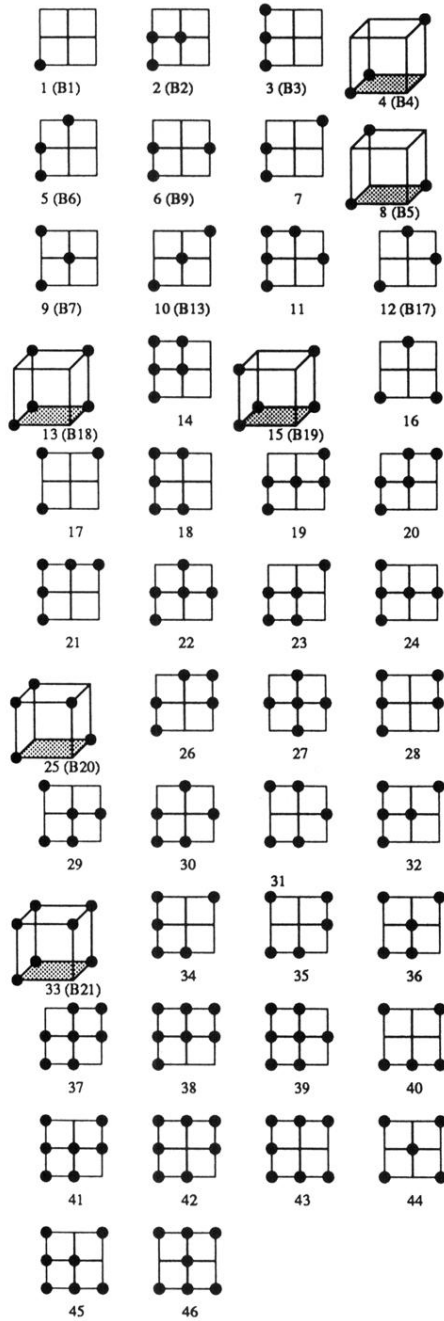


FIG. 2. Forty-six odd operators are shown in the order in which they are used in the MCRG analysis. In parenthesis we show the operators in common with Ref. 2.